CHEMISTRY
A EUROPEAN JOURNAL

DOI: 10.1002/chem.200902553

Transition-State Stabilization by a Secondary Substrate–Ligand Interaction: A New Design Principle for Highly Efficient Transition-Metal Catalysis

Tomáš Šmejkal, Denis Gribkov, Jens Geier, Manfred Keller, and Bernhard Breit*[a]

Abstract: A library of monodentate phosphane ligands, each bearing a guanidine receptor unit for carboxylates, was designed. Screening of the library gave some excellent catalysts for regioselective hydroformylation of β,γ-unsaturated carboxylic acids. A terminal alkene, but-3-enoic acid, was hydroformylated with a linear/branched (l/b) regioselectivity up to 41. An internal alkene, pent-3-enoic acid was hydroformylated with regioselectivity up to 18:1. Further substrate selectivity (e.g., acid vs. methyl ester) and reaction site selectivity (monofunctionalization of 2-vinylhept-2-enoic acid) were also achieved. Exploration of the structure–activity relationship and a practical and theoretical mechanistic study gave us an insight into the nature of the supramolecular guanidinium–carboxylate interaction within the catalytic system. This allowed us to identify a selective transition-state stabilization by a secondary substrate–ligand interaction as the basis for catalyst activity and selectivity.

Keywords: enzyme mimics · guanidine · homogeneous catalysis · hydroformylation · molecular recognition

Introduction

The application of supramolecular chemistry to catalysis has been a long-term objective of many research and development groups, with the ultimate goal being to produce supramolecular systems capable of mimicking the catalytic ability of natural enzymes. Pauling described enzymes as "molecules that are complementary in structure to the activated complex of the reaction that they catalyze" and therefore stabilize the transition state with respect to the uncatalyzed reaction.[1] The net result is a reaction rate enhancement and energetic differentiation among competing reaction pathways leading to isomeric products (selectivity).

A seemingly simple idea of how to make current synthetic catalysts more efficient and selective is to equip them with molecular recognition functionalities that can reversibly bind and orientate the substrate through noncovalent or reversible covalent interactions. In spite of recent progress in supramolecular catalysis, examples of successful catalyst design of this type are still relatively rare.[2] In our preliminary report, we recently described a new receptor-based phosphane ligand **1** (Scheme 1a), which furnishes a highly reactive and selective catalyst for regioselective hydroformylation of β,γ-unsaturated carboxylic acids (Scheme 1c).[2a]

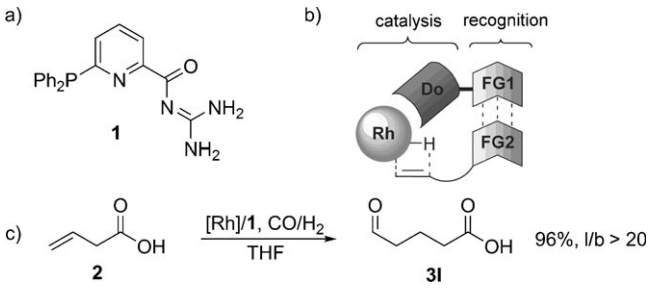

Scheme 1. a) Structure of ligand **1**.[2a] b) Concept of a supramolecular hydroformylation catalyst (Do = donor; FG1,2 = complementary functional groups). c) Regioselective hydroformylation of but-3-enoic acid (**2**).[2a]

Herein, we present a full account of our research on guanidine-based receptor ligands and their application in regioselective hydroformylation of β,γ-unsaturated carboxylic acids. Modifications of the ligand structure, a study of the structure–activity relationship and a theoretical study of the reaction mechanism are described. Recent applications of these ligands in decarboxylative hydroformylation of α,β-unsaturated carboxylic acids[2b] and activation of an aldehyde

[a] T. Šmejkal, D. Gribkov, J. Geier, M. Keller, B. Breit
Institut für Organische Chemie und Biochemie,
Freiburg Institute for Advanced Studies (FRIAS),
Albert-Ludwigs-Universität Freiburg,
Albertstrasse 21, 79104 Freiburg (Germany)
Fax: (+49) 761-2038715
E-mail: bernhard.breit@organik.chemie.uni-freiburg.de

Supporting information for this article is available on the WWW under http://dx.doi.org/10.1002/chem.200902553.

substrate function[3] are not included, and will be reported in full detail elsewhere.

Results and Discussion

Catalyst design: Our strategy was to combine the structural features of phosphane ligands (catalyst binding unit) with a guanidinium-based recognition site for carboxylates[4] in one ligand molecule (Scheme 2). The recognition unit should

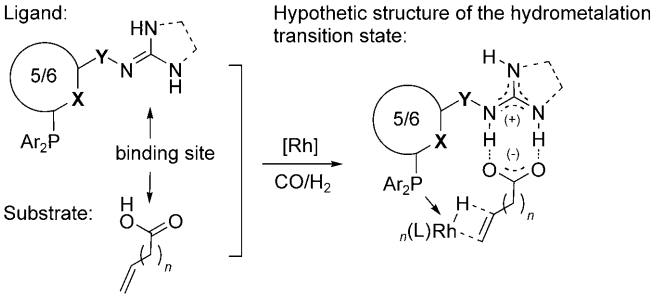

Scheme 2. Design of guanidine ligands for supramolecular catalysis, generalized structure of ligand (**X** = N, CH, NH; **Y** = CO, CH_2, or no linker) and substrate. Hypothetical structure of the hydrometalation transition state.

allow for substrate binding and conformational orientation. A further requirement of the design is that the ligand geometry should exactly match the transition-state structure. Only when the substrate–ligand interaction within the transition state is stronger than that in the catalyst–substrate adduct will lowering of the activation energy barrier (relative to the nonrecognition catalyst) be expected. By employing molecular modeling, some ligand geometries could be directly excluded, however, final tuning of the catalyst structure relied, to some extent, on trial and error. To lower the risk of failure, we adopted a strategy that has been frequently employed in medicinal chemistry and prepared not only a single ligand, but a small library of structurally diverse ligand molecules based on the design principle depicted in Scheme 2.

Hydroformylation of alkenes was selected as an ideal catalytic reaction to test our supramolecular catalytic system. Hydroformylation represents an example of an atom-economic C–C bond forming reaction that tolerates nearly all additional functional groups in the substrate molecule. Furthermore, this reaction constitutes the largest volume application of homogeneous metal catalysis in industry.[5] One possible drawback could be the multistep nature of the reaction. However, extensive mechanistic studies on a number of systems has revealed that, for rhodium triarylphosphane complexes, alkene hydrometalation is typically the rate- and selectivity-determining step.[6] Accordingly, control of this early step in the catalytic cycle should result in a large overall supramolecular effect.

Ligand synthesis: Synthesis of ligands is typically based on several building blocks, in particular, triarylphosphanes containing an amine or carboxylic acid function. Compounds such as **1** and **6–8** (Schemes 1 and 3), containing various core (pyridine, benzene, pyrrole) and binding site structures (acyl guanidine, acyl aminopyridine), have already been described.[2a,b,3]

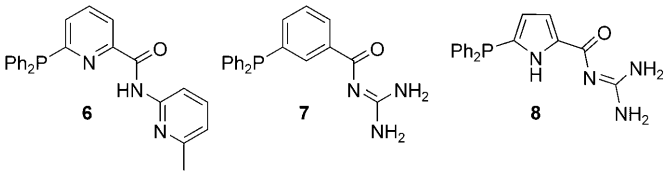

Scheme 3. Previously reported ligands **6**,[2a] **7**,[2a] and **8**.[3]

By using a similar synthetic strategy, carboxylic acids **9**[7] and **11**[8] were coupled with mono-Boc-protected (Boc = *tert*-butyloxycarbonyl) guanidine. In the next step, the protecting group was cleaved with trifluoroacetic acid to give, after neutralization, *ortho*-substituted ligand **10** and an electronically modified pyridine derivative **12** (Scheme 4).

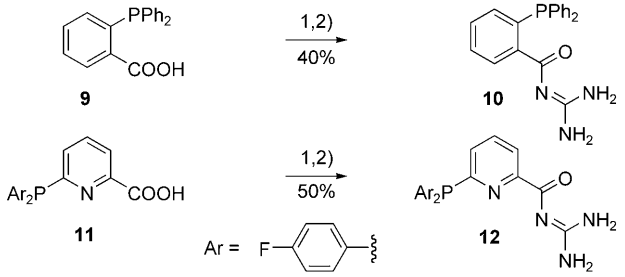

Scheme 4. Synthesis of ligands **10** and **12**: 1) Boc-guanidine (Boc = *tert*-butoxycarbonyl), *N*-methylmorpholine, 1-benzotriazolyloxytris(dimethylamino)phosphonium hexafluorophosphate, DMF, RT; 2) trifluoroacetic acid, RT, then Na_2CO_3, H_2O, CH_2Cl_2.

Introduction of the cyclic guanidine directing group was achieved by reaction of 2-aminoimidazoline toluene-*p*-sulfonate (**15**) with either the corresponding methyl picolinate **13** or methyl benzoate **14** precursors in methanol, in the presence of sodium methoxide as a base (Scheme 5).[9] While the methyl picolinate reacted to give **16** in good yield (75%), the yield of the methyl benzoate derivative **17** was lower (40%), presumably due to reduced electrophilicity.

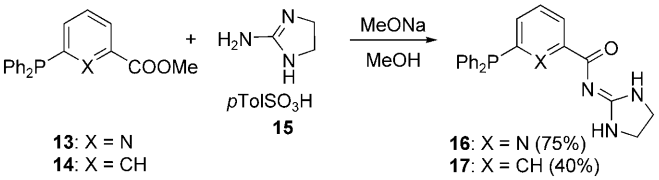

Scheme 5. Synthesis of ligands **16** and **17**.

Ligands in which the guanidinium group is attached either directly or through a CH_2 bridge to the triarylphosphane moiety were prepared by the reaction of the corresponding amine with 1-carbomethoxy-2-methylthio-2-imidazoline (**18**; Scheme 6).[10] Importantly, the methoxycarbonyl group was already cleaved under the reaction conditions.

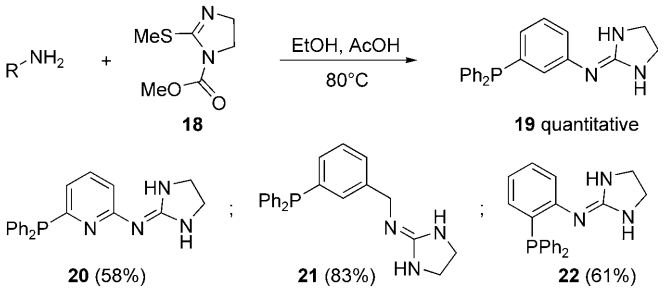

Scheme 6. Synthesis of ligands **19**, **20**, **21**, and **22**.

Hydroformylation of β,γ-unsaturated carboxylic acids: With the ligand library in hand, we started to evaluate its effectiveness in hydroformylation. As the first test system, hydroformylation of vinylacetic acid (**2**) was studied (Figure 1). The standard industrially applied catalyst, $[Rh(acac)(CO)_2]$/PPh_3 (acac = acetylacetone), displayed rather low activity (turnover frequency (TOF) = 30 h^{-1}, upper chart), and a typical linear/branched (l/b) regioselectivity (l/b = 1.3, lower chart). When the reaction was conducted with unmodified rhodium catalyst (no ligand added), moderate selectivity for the formation of the branched regioisomer (l/b = 0.6) was observed. Ligands **10** and **22**, which are equipped with a receptor moiety in the *ortho*-position relative to the phosphane moiety, inhibited the reaction completely. This may be a possible consequence of rhodium chelation between these two functionalities.

Activity and selectivity comparable to that with PPh_3 was observed for the majority of ligands tested (**19**, **16**, **20**, **17**, **6**, **21**, and **7**). However, three acylguanidine derivatives (**1**, **8**, and **12**) gave catalysts with much higher activity. Pyridylacylguanidinium ligand **1** gave an outstanding catalyst that operated with excellent activity (TOF = 250 h^{-1}) and regioselectivity (l/b = 23). Interestingly, the activity and selectivity could be further improved by fine-tuning of the electronic properties of the ligand. Derivative **12**, bearing two fluoro-substituents, gave even higher regioselectivity (l/b = 41) with TOF > 350 h^{-1}.[11] On the other hand, in the hydroformylation of but-3-enoic acid (**2**), although pyrrole derivative **8** provided one of the highest reaction rates (TOF = 286 h^{-1}), unfortunately, the regioselectivity was low (l/b = 3.5). Apparently, the formation of both regioisomers is promoted to similar extents with this ligand. The most active catalysts identified during the screening were applied in a more challenging reaction: the hydroformylation of internal alkene (*Z*)-pent-3-enoic acid (**23**; Table 1). When using triphenylphosphane as a ligand, hydroformylation proceeded sluggishly; under these conditions, the catalyst produced 5.5 equivalents of aldehyde products in 68 h and formation of **25** over **24** was only slightly preferred (Tabel 1, entry 1). In contrast, an unprecedentedly high regioselectivity in the hydroformylation of an internal alkene was achieved by using ligand **1**; in this case, branched aldehyde **24** was obtained as the major reaction product (**24**/**25** = 11:1; Table 1, entry 2) together with increased conversion (TON = 39). Applying more reactive catalysts based on ligands **12** and **8** allowed lower catalyst loadings (1 mol% [Rh]) to be used and reduced the reaction time (20 h). Ligand **12** also gave the highest regioselectivity (**24**/**25** = 18.1:1; Table 1, entry 3).

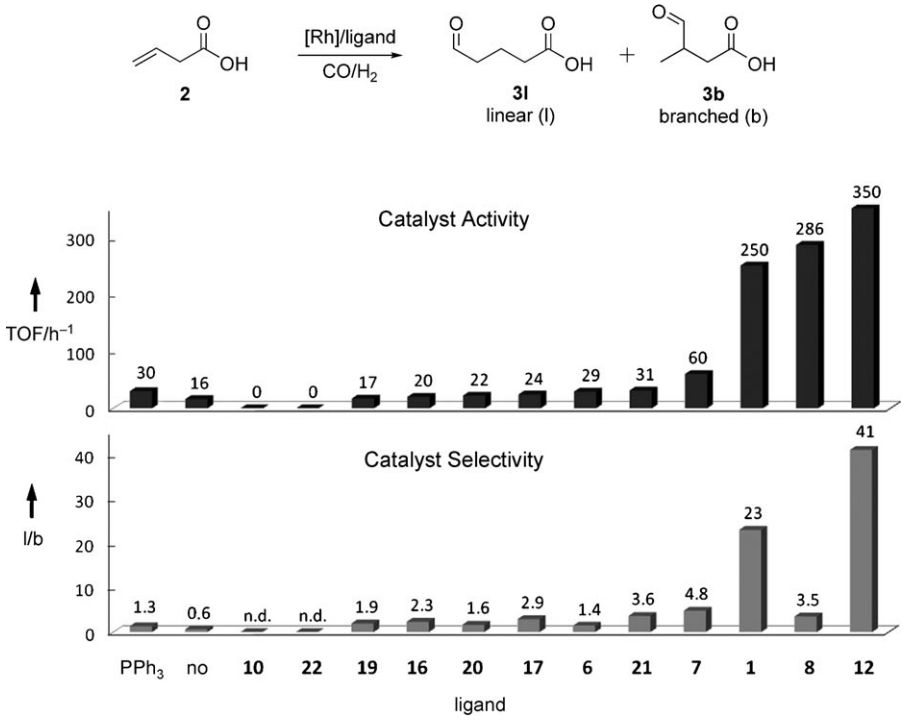

Figure 1. Hydroformylation of **2**; $[Rh(acac)(CO)_2]$/ligand/**2** = 1:10:200 (acac = acetylacetonate); c_0(**2**) = 0.2 M, THF (2 mL), 10 bar CO/H_2 (1:1), 40 °C, 4 h. TOF (mole aldehyde per mole catalyst per hour) determined from the gas consumption curve. Regioselectivity, linear/branched (l/b) ratio, was determined by ^1H NMR spectroscopic analysis of the reaction mixture. n.d. = not determined.

Furthermore, the directed hydroformylation was applied in selective monofunctionalization of substrate **26**, bearing two terminal double bonds of similar reactivity. Hydroformylation of

Table 1. Hydroformylation of (*Z*)-pent-3-enoic acid (**23**).

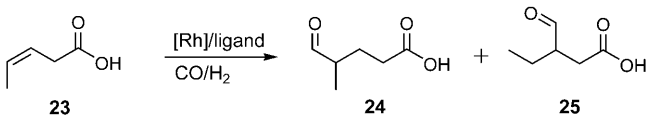

23 **24** **25**

Entry	Ligand	Time [h]	TON[a]	Regioselectivity [**24**/**25**]
1[b]	PPh_3	68	5.5	1:1.7
2[b]	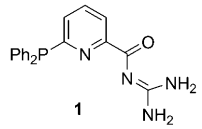 **1**	68	39	11:1
3[c]	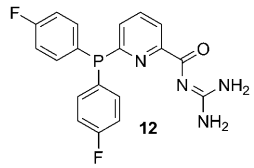 **12**	20	73	18.1:1
4[c]	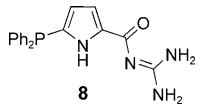 **8**	20	93	3.9:1

[a] Turnover number = TON (mole of aldehydes per mole catalyst); [b] [Rh(acac)$(CO)_2$]/ligand/**23** = 1:10:50, c_0(**23**) = 0.2 M, THF (4 mL), 6 bar CO/H_2 (1:1), RT, 68 h; [c] [Rh(acac)$(CO)_2$]/ligand/**23** = 1:10:100, c_0(**23**) = 0.2 M, THF (2 mL), 10 bar CO/H_2 (1:1), 40 °C, 20 h.

26 can potentially give up to four regioisomeric mono-aldehydes (**27**–**30**) and four bis-aldehydes (**31**) six of them as a mixture of two or more diastereoisomers (Scheme 7).

When using triphenylphosphane as a ligand, the rates of hydroformylation of the two alkene functions were very similar (see Figure 2, which displays ^{1}H NMR spectra of aliquots taken from the reaction mixture at different reaction times and highlights the similar rates of alkene consumption). Regardless of when the reaction was stopped, we obtained an intractable mixture of several mono- and dihydroformylated products (**27**–**31**).

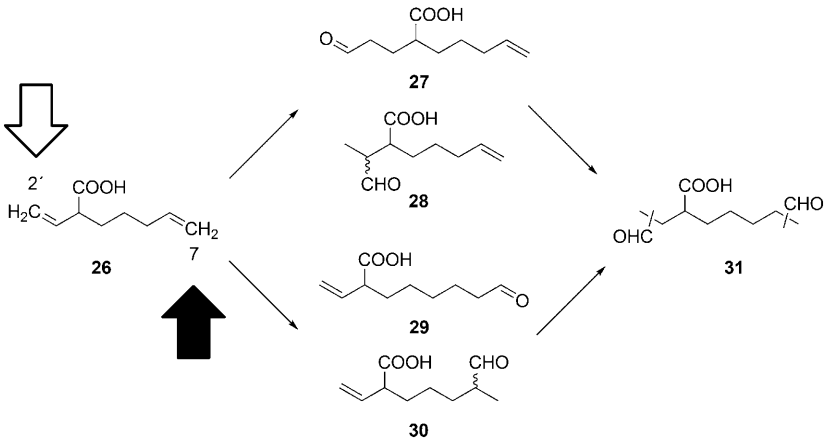

Scheme 7. Hydroformylation of **26**; [Rh(acac)$(CO)_2$]/ligand/**26** = 1:10:150; c_0(**26**) = 0.2 M, THF (8 mL), 4 bar CO/H_2 (1:1), 25 °C.

When using ligand **1**, the remote alkene functional group was hydroformylated at a similar rate and selectivity (l/b) to that with PPh_3. Conversely, the β,γ-alkene group reacted ten times faster (compared with PPh_3) in a highly regioselective manner, which is again indicative of a directed process (see Figure 3, which displays ^{1}H NMR spectra of aliquots taken from the reaction mixture at different reaction times and highlights the reaction-site selectivity). On a preparative scale, aldehyde **27** could be isolated in 75% yield.[8]

Hydroformylation of γ,δ-unsaturated carboxylic acids: Hydroformylation of the homologue pent-4-enoic acid (**32**), which has the double bond one carbon further removed from the carboxylate, was attempted (Figure 4). However, most of the ligands tested showed reactivity comparable to that of triphenylphosphane. Pyrrole derivative **8** was the only ligand for which a significant supramolecular effect was observed; in this case the rate enhancement was approximately fivefold higher than that with PPh_3 (TOF = 125 h^{-1}, l/b = 7.3:1).

The observed selectivity is surprising at first sight. Given that addition of the formyl group occurred mainly at C-4 for the β,γ-unsaturated substrates **2** and **23**, one would expect a high selectivity for the formation of branched product **24**. However, although the identical alkyl rhodium intermediate **34** (see Scheme 8) could be formed from both substrates **23** and **32**, the transition-state structures of the corresponding hydrometalation steps leading to this common intermediate are different. Clearly, the catalyst is not able to efficiently accommodate any of the alternative hydrometalation transition states of the γ,δ-unsaturated substrate **32**. Taken together, these results provide evidence for hydrometalation being the rate- and selectivity-determining step (see below).

Control experiments: The proposed reaction mechanism, including supramolecular ligand–substrate interaction, was supported by a number of control experiments. No supramolecular effect was observed for ligand **35**, which bears a protected guanidine (Table 2, entry 2). Furthermore, when a combination of acylguanidine **36** and triphenylphosphane was used, neither the desired activity nor selectivity were obtained (Table 2, entry 3). These findings suggest that the molecular recognition and catalytic units must be an integral part of the same molecule to achieve the enhanced catalytic activity and selectivity. Further evidence came from the fact that methyl ester **37**, which lacks the complementary acid functionality, reacted slowly and with low selectivity (Table 2, entries 4 and 5).

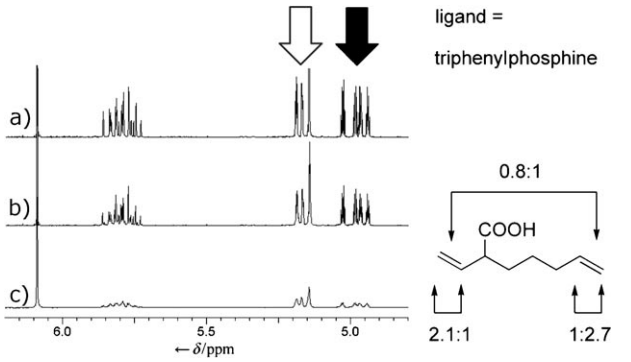

Figure 2. Hydroformylation of **26** using PPh_3 as a ligand. ^{1}H NMR spectra (400 MHz, $CDCl_3$) of the double-bond region: a) 0 h; b) 9.5 h; c) 25.3 h. Signals from H-2′ and H-7 are marked with empty and filled arrows, respectively. Reaction-site selectivity and regioselectivity were determined by ^{1}H NMR spectroscopic analysis of the reaction mixture.

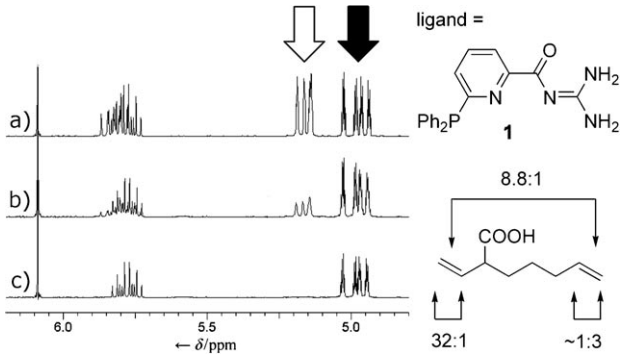

Figure 3. Hydroformylation of **26** using ligand **1**. ^{1}H NMR spectra (400 MHz, $CDCl_3$) of the double-bond region: a) 0 h; b) 4 h; c) 8.5 h. Signals from H2′ and H7 are marked with empty and filled arrows, respectively. Reaction-site selectivity and regioselectivity were determined by ^{1}H NMR spectroscopic analysis of the reaction mixture.

Furthermore, using a catalyst containing a molecular recognition unit should make substrate differentiation possible, which would be difficult to achieve with classical catalysts. Thus, we carried out a competition experiment in which a 1:1 mixture of terminal olefins of similar reactivity was hydroformylated in the presence of [Rh(acac)(CO)$_2$]/**1** catalyst (Table 3). The ratio of products at low conversion indicates that the reaction rate of the hydroformylation of noncomplementary substrates was considerably slower and the corresponding aldehyde products were formed without any regioselectivity (l/b ratio = 2.3–3). Thus, our supramolecular catalyst can carry out a chemical transformation selectively on a specific target in a mixture of chemical substances.

If the interaction between the carboxylic acid and the guanidine is important for catalyst performance, the addition of a second carboxylic acid to the reaction medium should lead to competition for the recognition site. Indeed, when acetic acid was added to the reaction mixture (1–5 equiv relative to **2**), we observed inhibition and decreased selectivity (Figure 5).[12] These experimental results also exclude the possibility that the carboxylic acid simply functions as a template for supramolecular bidentate ligand formation, which could result in selectivity for the linear product.

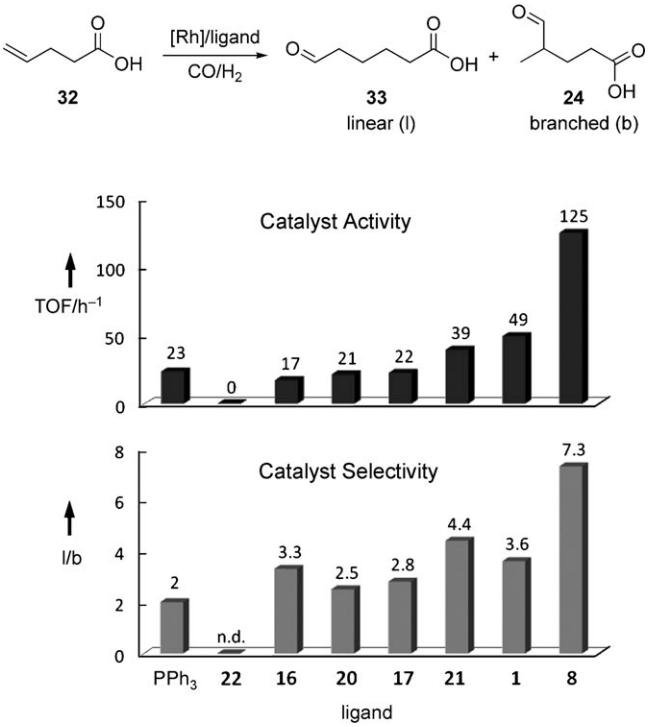

Figure 4. Hydroformylation of **32**. [Rh(acac)(CO)$_2$]/ligand/**32** = 1:10:200, c_0(**32**) = 0.2 M, THF (2 mL), 10 bar CO/H$_2$ (1:1), 40 °C, 4 h. TOF (mole aldehyde per mole catalyst per h^{-1}) determined from the gas consumption curve. Regioselectivity (**33**/**24** ratio) was determined by ^{1}H NMR spectroscopic analysis of the reaction mixture. n.d. = not determined.

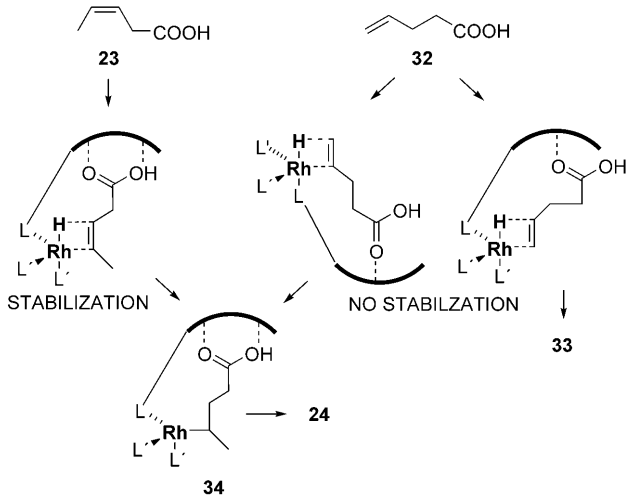

Scheme 8. Substrate binding in the rate- and selectivity-determining hydrometalation step for substrates **23** and **32**. The bold curve represents the substrate binding site of ligand **1**.

A mechanism in which the recognition event precedes the catalytic reaction implies that, for high substrate concentrations, saturation should be achieved. Hydroformylation of **2** was therefore conducted at various substrate concentrations

Table 2. Control experiments.[a]

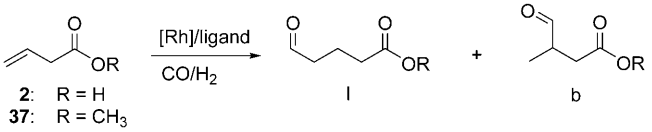

ligands:

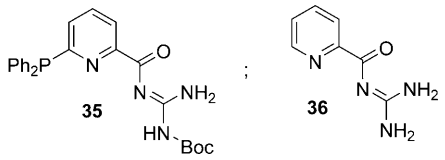

Entry	Ligand	Substrate	Conversion [%]	Regioselectivity [l/b ratio]	TOF [h^{-1}]
1	**1**	**2**	100	23	250
2	**35**	**2**	77	1.4	50
3	PPh_3/**36** (1:1)	**2**	20	1.5	12
4[b]	**1**	**37**	50	1.1	29
5	**1**	**37**/AcOH (1:1)	58	1.4	34

[a] [Rh(acac)$(CO)_2$]/ligand/substrate = 1:10:200, c_0(substrate) = 0.2 M, THF (2 mL), 10 bar CO/H_2 (1:1), 40 °C, 4 h; [b] Suspension (ligand **1** is practically insoluble in the reaction medium without a carboxylic acid); all other runs were clear solutions.

Table 3. Hydroformylation of a 1:1 mixture of two substrates.[a]

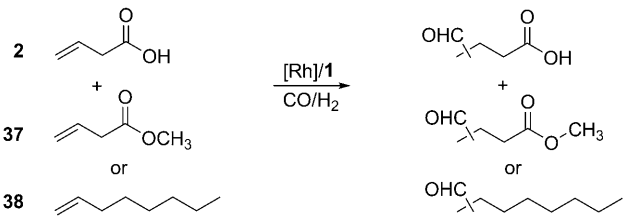

Entry	Substrate	Relative rate of hydroformylation	Regioselectivity [l/b ratio]
1	**2**	1	50
2	**37**	< 0.1	2.3
3	**38**	< 0.15	3

[a] [Rh(acac)$(CO)_2$]/**1**/**2**/**37**(**38**) = 1:20:200:200, c_0(**2**) = c_0(**37** or **38**) = 0.13 M, THF (6 mL), 4 bar CO/H_2 (1:1), RT.

(0.05–0.4 M). Indeed, substrate saturation and even inhibition was observed.[8]

All these results are consistent with a reaction mechanism analogous to enzyme catalysis: 1) binding of the substrate to the ligand(s) of the rhodium phosphane complex; 2) directed catalytic reaction within the supramolecular substrate–catalyst complex. However, the most important questions still remain to be answered: What does the catalyst–substrate complex look like and what is the source of the reaction selectivity? Hence, we decided to study the mechanism of vinylacetic acid (**2**) hydroformylation in more detail.

Reaction mechanism: By using the activity and selectivity data (Figure 1), the relative reaction rates for the formation of linear aldehyde **3l** (v_L(rel)) and branched aldehyde **3b** (v_B(rel)) with either the [Rh]/**1** catalyst or the [Rh]/PPh_3 catalyst were calculated (Figure 6).[13] Differences in the relative rate of formation of the branched isomer **3b** (v_B(rel)] are minimal (Table 4). Accordingly, the energy of the branched transition state does not seem to be particularly affected by the secondary catalyst–ligand interaction. In contrast, the relative rate of formation of the linear isomer **3l** (v_L(rel)) is 14-times faster for the catalyst [Rh]/**1** than for [Rh]/PPh_3; this acceleration is thus the source of the reaction selectivity (Table 4).

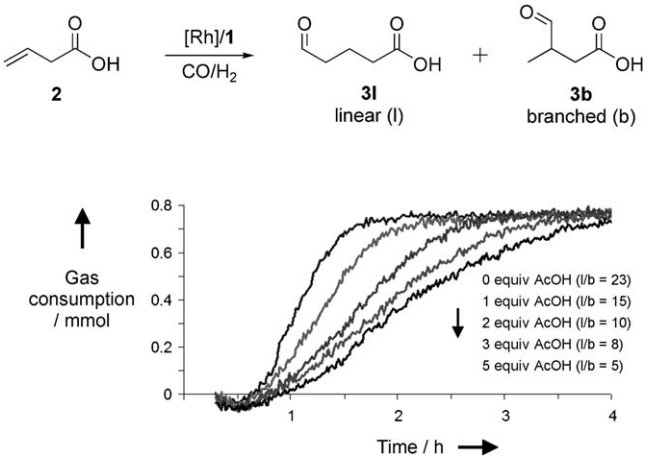

Figure 5. Hydroformylation of **2**; [Rh(acac)$(CO)_2$]/**1**/**2**/AcOH = 1:10:200:(0–1000), c_0(**2**) = 0.2 M, THF (2 mL), 10 bar CO/H_2 (1:1), 40 °C, 4 h. Gas consumption curves for increasing amounts of inhibitor AcOH (0–5 equiv relative to substrate **2**). Regioselectivity (l/b ratio) was determined by ^{1}H NMR spectroscopic analysis of the reaction mixture.

Table 4. Effect of molecular recognition on the reaction rate.[a]

Ligand	v_L(rel)	v_B(rel)
PPh_3	1	0.77
1	14.13	0.61

[a] Reagents and conditions, see Figure 1. v(rel) = rate of hydroformylation (aldehyde formation) relative to v_L(rel, PPh_3).

Clearly, the supramolecular interaction matches the transition-state requirements for the formation of the linear regioisomer and lowers the activation energy relative to the nonrecognition catalyst. This is schematically demonstrated in Figure 6, which shows selective lowering of the energy barriers by an amount relating to the strength of the supramolecular ligand–substrate interaction.[14]

To gain a deeper understanding of the reaction, several NMR spectroscopy experiments were undertaken with the catalyst precursor [Rh(acac)$(CO)_2$] and two equivalents of ligand **1**, suspended in $CDCl_3$ under argon. After addition of AcOH (1.0 equiv), dissolution of the compounds was observed and the mixture was analyzed by NMR spectroscopy. However, only very broad ^{1}H and ^{31}P NMR signals were observed and no signal assignments were possible. After addition of three further equivalents of AcOH, much clearer spectra were observed. The spectra were interpreted as arising from the rhodium carboxylate complex **39** [Rh(**1**)$_2$(CO)OAc] (Scheme 9) by analogy to the known tri-

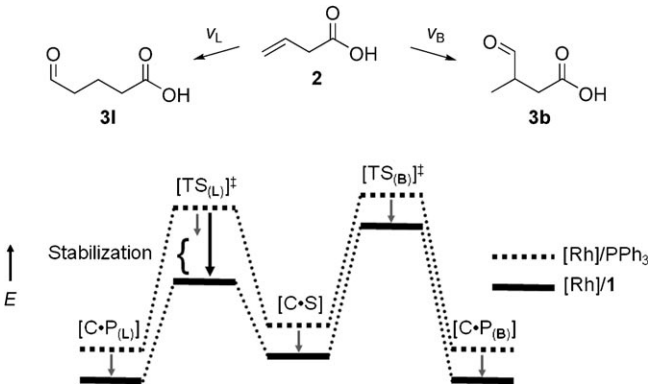

Figure 6. Energy surfaces for the catalyst without (dashed) or with (full) a molecular recognition system. Stabilization imparted by supramolecular interaction marked with arrows, [C·S] or [C·P] represents catalyst–substrate (product) adduct, $[TS_{(L)}]^{+}$ and $[TS_{(B)}]^{+}$ represent the corresponding transition states. Selective lowering of the energy barrier is marked with a black parenthesis.

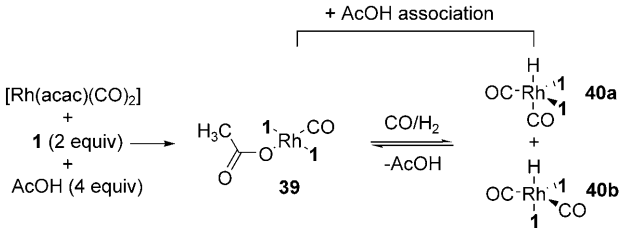

Scheme 9.

phenylphosphane complex *trans*-$[Rh(CO)OAc(PPh_3)_2]$.[15] Additionally, no signal was observed in the typical rhodium hydride region of the ^{1}H NMR ($\delta = -9$ to -10 ppm). When high-pressure NMR spectroscopy was used to investigate the effect of CO/H_2 pressure (1:1; 10–40 bar) on this complex, the formation of characteristic signals of rhodium hydride species (^{1}H NMR: $\delta = -9.2$ to -9.6 ppm) was observed. However, the broad nature of the ^{1}H and ^{31}P NMR signals did not enable unequivocal identification of the corresponding complexes. By analogy to known triphenylphosphane complexes,[16] formation of the rapidly equilibrating trigonal bipyramidal isomers **40a** and **40b** is proposed (Figure 6). Complexes **39** and **40** thus represent the resting state of the active hydroformylation catalyst.

For solubility reasons, determination of the ligand–substrate association constant had to be carried out in $[D_6]$DMSO. Nevertheless, based on ^{1}H NMR spectroscopic titration experiments and spectroscopic studies of model systems (picrate, trifluoracetate), a complete association system of acetic acid and **1** could be constructed (Scheme 10).[8] Thus, a solution of the free base **1** was titrated with tetramethyl ammonium acetate (AcO^-) and the shift changes of the ^{1}H NMR signals associated with the ligand protons were monitored. Good fit of the measured data with the theoretical model for association constant $K_{ass} = 430\,M^{-1}$ with a 1:1 stoichiometry was obtained (Scheme 10a). Accordingly, the hypothetical association constant of protonated ligand $\mathbf{1}^+$/AcO^- should be greater than $430\,M^{-1}$ because of the additional attractive interaction between the opposite charges (Scheme 10b). Titration of the free base **1** with acetic acid (0–24 equiv) caused a significant downfield shift of various proton signals of **1** in the ^{1}H NMR spectrum. Interestingly, comparison of these spectra with spectra obtained after the addition of one equivalent of either CF_3COOH or picric acid revealed that signals of all protons of **1** gradually shifted towards those of the protonated ligand $\mathbf{1}^+$. This is interpreted as a gradual protonation of **1** (approximate equilibrium constant of this process is $K_{eq} = 0.7\,M^{-1}$, Scheme 10c).

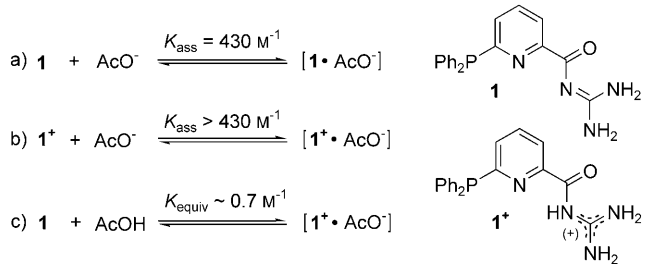

Scheme 10. NMR study of **1**/AcOH interaction {[D6]DMSO, 300 MHz, $c_0(\mathbf{1}) = 0.02$–$0.03\,M$, RT}.[8]

In conclusion, these experiments suggest that, due to the relatively low basicity of the acylguanidine **1**, both protonated ($\mathbf{1}^+$) and neutral (**1**) ligands can coexist under the reaction conditions of hydroformylation catalysis and, furthermore, that both ligand forms are able to efficiently bind to carboxylates.

To get a better insight into the function of this catalyst system, we undertook theoretical studies (DFT) on what is considered to be the rate- and selectivity-determining step of the rhodium/phosphane-catalyzed hydroformylation, that is, the alkene hydrometalation[6] (Figure 7).[17] Interestingly, the originally envisioned two-point guanidinium–carboxylate interaction mode (Scheme 2) could not be localized as an energy minimum, probably due to a severe repulsion between the lone electron pairs of the pyridine nitrogen and the carboxylate oxygen.[18] However, the most stable catalyst–substrate complex conformation (Figure 7a) was found to involve the carboxylate complexed by four hydrogen bonds from both guanidine ligands (one protonated, one neutral). Interestingly, even for this intermediate, the calculated conformation predicts that the alkene should be significantly turned from the P–Rh–P plane of the trigonal bipyramidal complex towards that of the transition state leading to the linear alkyl rhodium intermediate. On the way to the transition state the alkene moiety rotates further out of the equatorial plane and the hydride is transferred from the metal center to the alkene moiety (Figure 7b). The calculation indicates an early transition state containing a nearly unperturbed rhodium–hydride bond (Rh–H bond lengthens by only 0.065 Å). According to this analysis, most of the activation energy for the hydrometalation can be attributed to the rotation of the alkene from the equatorial in-plane arrangement in the reactant to a nearly perpendicular orienta-

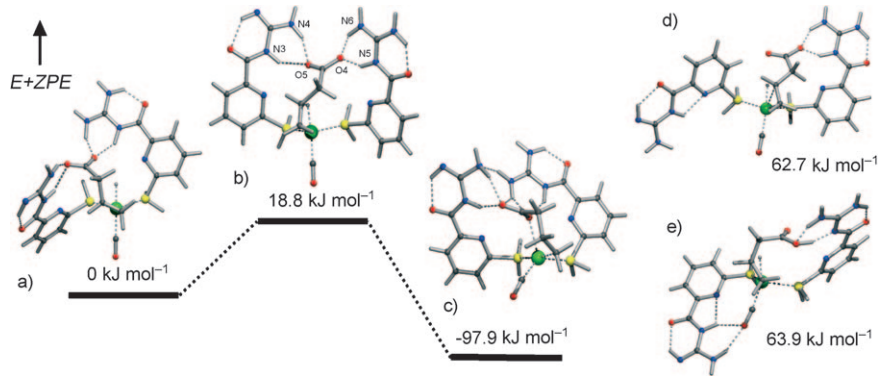

Figure 7. DFT calculations on the reaction mechanism of directed hydroformylation of **2**. a) Catalyst–substrate complex; b) transition state of hydrometalation; c) catalyst–product complex; d, e) alternative transition states. $E+ZPE$ = electronic energy + zero point energy (relative to structure **a**).

tion in the transition state. This movement is assisted by a supramolecular interaction, which becomes optimal at the transition state with hydrogen bonds pointing directly toward the lone pairs of the carboxylate (d(N3–H···O5) = 2.012 Å, d(N4–H···O5) = 1.857 Å, d(N5–H···O4) = 1.569 Å, d(N6–H···O4) = 1.583 Å). This binding motif closely resembles the so-called "oxanion hole" structures that are known in enzymes and clearly stabilizes the formation of the carboxylate anion.[19] Additionally, this coordination mode minimizes repulsion between the lone pair of the pyridine nitrogen and the anionic carboxylate oxygen. For the hydrometalation product (alkyl rhodium intermediate), the calculation predicts a complex network of hydrogen bonding both between the ligand and the substrate and also between ligands (Figure 7c). Additionally, a rhodium–carboxylate interaction (d(Rh···O) = 2.463 Å) was also identified. All attempts to find an alternative catalyst–substrate interaction mode (e.g., one ligand bonding as shown in Figure 7d; or hydrogen bonding only as shown in Figure 7e) resulted in much higher activation energies.

Although the hydrometalation step is supposed to be rate- and selectivity-determining, the catalytic cycle cannot be reduced to this step only. The system based on the monodentate receptor ligands is quite flexible and the binding geometry may vary during the catalytic cycle to accommodate further reaction intermediates. The guanidine ligand might also participate in CO dissociation (see Figure 7e), alkene coordination or the hydrogenolysis of the acyl–rhodium intermediate.

Conclusion

A library of phosphane ligands bearing guanidine receptor units for carboxylates was prepared and tested in the hydroformylation of unsaturated carboxylic acids. This study has led to the identification of some new ligand structures that could even surmount the activity and selectivity of the originally published supramolecular catalyst [Rh]/**1**. Notably, a direct comparison of the performance of various catalysts has enabled us to draw important conclusions concerning structure–activity relationships. A mechanistic study of one particular case—regioselective hydroformylation of **2**—revealed that the experimentally observed enhancement in activity and selectivity brought about by the ligand is a result of the selective supramolecular transition-state stabilization within our system. Furthermore, the transition-state geometry and the nature of the supramolecular catalyst–substrate interaction were identified by using DFT calculations. These calculations have led to a refinement of our originally proposed supramolecular interaction geometry and enabled a better understanding of the factors involved in transition-state stabilization.

We hope that a detailed understanding of the reaction mechanism will encourage future designs of supramolecular and biomimetic catalysts for a broad variety of synthetically relevant transformations.

Experimental Section

General procedure for hydroformylation experiments: Experiments were performed either in a Premex stainless steel autoclave Medimex (100 mL) equipped with a glass liner containing a magnetic stirring bar (1000 rpm) or in an Argonaut Endeavour reactor system consisting of eight parallel mechanically stirred (500 rpm) pressure reactors with individual temperature and pressure controls. The hydroformylation solution was prepared by charging a Schlenk flask with [Rh(acac)(CO)$_2$], ligand, 1,3,5-trimethoxybenzene (internal standard ^{1}H NMR) and solvent, under argon. Then, the substrate was added and the mixture was stirred for 5 min under argon. The solution was transferred to the autoclave with a syringe under an argon atmosphere. The autoclave was purged three times with synthesis gas CO/H$_2$ (1:1) and the reaction was conducted as specified in the text. Runs were stopped by cooling the system (if appropriate), venting, and purging with argon. Reaction kinetics were monitored either from the gas consumption curve or by ^{1}H NMR spectroscopic analysis of reaction samples.

Acknowledgements

This work was supported by the Fonds der Chemischen Industrie, the Deutsche Forschungsgemeinschaft (GRK 1038), and an Alfried Krupp Award for young university teachers of the Krupp foundation (to B.B.).

[1] a) L. Pauling, *Nature* **1948**, *161*, 707–709; b) A. Warshel, P. K. Sharma, M. Kato, Y. Xiang, H. Liu, M. H. M. Olsson, *Chem. Rev.* **2006**, *106*, 3210–3235.

[2] a) T. Šmejkal, B. Breit, *Angew. Chem.* **2008**, *120*, 317–321; *Angew. Chem. Int. Ed.* **2008**, *47*, 311–315; b) T. Šmejkal, B. Breit, *Angew. Chem.* **2008**, *120*, 4010–4013; *Angew. Chem. Int. Ed.* **2008**, *47*, 3946–3949; c) T. E. Lightburn, M. T. Dombrowski, K. L. Tan, *J. Am.*

Chem. Soc. **2008**, *130*, 9210–9211; d) C. U. Grünanger, B. Breit, *Angew. Chem.* **2008**, *120*, 7456–7459; *Angew. Chem. Int. Ed.* **2008**, *47*, 7346–7349; e) M. D. Pluth, R. G. Bergman, K. N. Raymond, *Science* **2007**, *316*, 85–88; f) S. Das, C. D. Incarvito, R. H. Crabtree, G. W. Brudvig, *Science* **2006**, *312*, 1941–1943; g) F. Goettmann, P. Le Floch, C. Sanchez, *Chem. Commun.* **2006**, 2036–2038; h) D. B. Grotjahn, *Chem. Eur. J.* **2005**, *11*, 7146–7153; i) J. Yang, B. Gabriele, S. Belvedere, Y. Huang, R. Breslow, *J. Org. Chem.* **2002**, *67*, 5057–5067; j) H. K. A. C. Coolen, J. A. M. Meeuwis, P. W. N. M. van Leeuwen, R. J. M. Nolte, *J. Am. Chem. Soc.* **1995**, *117*, 11906–11913.

[3] L. Diab, T. Šmejkal, J. Geier, B. Breit, *Angew. Chem.* **2009**, *121*, 8166–8170; *Angew. Chem. Int. Ed.* **2009**, *48*, 8022–8026.

[4] a) J. W. Steed, J. L. Atwood, *Supramolecular Chemistry*, Wiley, New York, **2000**; b) C. Schmuck, *Coord. Chem. Rev.* **2006**, *250*, 3053–3067.

[5] a) K. Weissermel, H.-J. Arpe, *Industrial Organic Chemistry*, Wiley-VCH, Weinheim, **2003**, pp. 127–144; b) B. Breit, W. Seiche, *Synthesis* **2001**, 1–36.

[6] a) E. Zuidema, L. Escorihuela, T. Eichelsheim, J. J. Carbó, C. Bo, P. C. J. Kamer, P. W. N. M. van Leeuwen, *Chem. Eur. J.* **2008**, *14*, 1843–1853; b) J. J. Carbó, F. Maseras, C. Bo, P. W. N. M. van Leeuwen, *J. Am. Chem. Soc.* **2001**, *123*, 7630–7637; c) S. A. Decker, T. R. Cundari, *J. Organomet. Chem.* **2001**, *635*, 132–141; d) *Rhodium-catalyzed hydroformylation* (Eds.: P. W. N. M. van Leeuwen, C. Claver), Kluver, Dordrecht, **2000**.

[7] a) J. E. Hoots, T. B. Rauchfuss, D. A. Wrobleski, *Inorg. Synth.* **1982**, *21*, 175–179.

[8] For details see the Supporting Information.

[9] D. E. Beattie, G. M. Dover, T. J. Ward, *J. Med. Chem.* **1985**, *28*, 1617–1620.

[10] S. R. Mundla, L. J. Wilson, S. R. Klopfenstein, W. L. Seibel, N. N. Nikolaides, *Tetrahedron Lett.* **2000**, *41*, 6563–6566.

[11] Less basic phosphanes typically afford higher activity and higher l/b ratios in hydroformylation: a) L. A. van der Veen, M. D. K. Boele, F. R. Bregman, P. C. J. Kamer, P. W. N. M. van Leeuwen, K. Goubitz, J. Fraanje, H. Schenk, C. Bo, *J. Am. Chem. Soc.* **1998**, *120*, 11616–11626; b) C. P. Casey, E. L. Paulsen, E. W. Buettenmueller, B. R. Proft, L. M. Petrovich, B. A. Matter, D. R. Powell, *J. Am. Chem. Soc.* **1997**, *119*, 11817–11825.

[12] Inhibition effect of carboxylic acids on the hydroformylation of hex-1-ene has been already described but the regioselectivity was unaffected. E. Mieczyńska, A. M. Trzeciak, J. J. Ziółkowski, *J. Mol. Catal.* **1993**, *80*, 189–200.

[13] Hydroformylation of **2**, Catalyst [Rh]/PPh_3: TOF = 30 h^{-1}, l/b = 1.3:1 $\Rightarrow \nu_L(\mathrm{rel,PPh_3}) = 1; \nu_B(\mathrm{rel,PPh_3}) = 1/1.3 = 0.77$ Hydroformylation of **2**, Catalyst [Rh]/**1**: TOF = 250 h^{-1}, l/b = 23:1. $\Rightarrow \nu_L(\mathrm{rel,}\mathbf{1}) = \frac{(250\times23)/24}{(30\times1.3)/2.3} = 14.13; \nu_B(\mathrm{rel,}\mathbf{1}) = \frac{(250\times1)/24}{(30\times1.3)/2.3} = 0.61$

[14] Compare: a) S. Das, G. W. Brudvig, R. H. Crabtree, *Chem. Commun.* **2007**, 1–24; b) S. Das, G. W. Brudvig, R. H. Crabtree, *J. Am. Chem. Soc.* **2008**, *130*, 1628–1637.

[15] Y. S. Varshavskii, T. G. Cherkasova, I. S. Podkorytov, A. A. Korlyukov, V. N. Khrustalev, A. B. Nikol'skii, *Russ. J. Coord. Chem.* **2005**, *31*, 121–131.

[16] J. M. Brown, A. G. Kent, *J. Chem. Soc. Perkin Trans. 2* **1987**, 1597–1607.

[17] The structures were optimized at the B3LYP/3-21G** level. Calculations were performed with the software package Gaussian 03. Gaussian 03, Revision B.04, M. J. Frisch, G. W. Trucks, H. B. Schlegel, G. E. Scuseria, M. A. Robb, J. R. Cheeseman, J. A. Montgomery, Jr., T. Vreven, K. N. Kudin, J. C. Burant, J. M. Millam, S. S. Iyengar, J. Tomasi, V. Barone, B. Mennucci, M. Cossi, G. Scalmani, N. Rega, G. A. Petersson, H. Nakatsuji, M. Hada, M. Ehara, K. Toyota, R. Fukuda, J. Hasegawa, M. Ishida, T. Nakajima, Y. Honda, O. Kitao, H. Nakai, M. Klene, X. Li, J. E. Knox, H. P. Hratchian, J. B. Cross, V. Bakken, C. Adamo, J. Jaramillo, R. Gomperts, R. E. Stratmann, O. Yazyev, A. J. Austin, R. Cammi, C. Pomelli, J. W. Ochterski, P. Y. Ayala, K. Morokuma, G. A. Voth, P. Salvador, J. J. Dannenberg, V. G. Zakrzewski, S. Dapprich, A. D. Daniels, M. C. Strain, O. Farkas, D. K. Malick, A. D. Rabuck, K. Raghavachari, J. B. Foresman, J. V. Ortiz, Q. Cui, A. G. Baboul, S. Clifford, J. Cioslowski, B. B. Stefanov, G. Liu, A. Liashenko, P. Piskorz, I. Komaromi, R. L. Martin, D. J. Fox, T. Keith, M. A. Al-Laham, C. Y. Peng, A. Nanayakkara, M. Challacombe, P. M. W. Gill, B. Johnson, W. Chen, M. W. Wong, C. Gonzalez, J. A. Pople, Gaussian, Inc., Wallingford CT, **2004**.

[18] Compare: C. Schmuck, U. Machon, *Chem. Eur. J.* **2005**, *11*, 1109–1118.

[19] D. Voet, J. G. Voet, *Biochemistry*, 2nd ed., Wiley, New York, **1995**.

Received: September 16, 2009
Published online: January 14, 2010

